Cajal Body dynamics and association with chromatin are ATP-dependent

Melpomeni Platani*, Ilya Goldberg†‡, Angus I. Lamond* and Jason R. Swedlow*§

*School of Life Sciences, Division of Gene Regulation and Expression, University of Dundee, Medical Sciences Institute/Wellcome Trust Biocentre, Dow Street, Dundee, DD1 5EH, Scotland

†Department of Biology, Massachusetts Institute of Technology, 77 Mass Avenue, Cambridge, MA 02139, USA

‡Current address: Laboratory of Genetics, National Institute on Aging, National Institutes of Health, 333 Cassell Drive, Suite 4000, Baltimore, MD 21224, USA

§e-mail: j.swedlow@dundee.ac.uk

Published online: 17 June 2002; DOI: 10.1038/ncb809

Cajal bodies (CBs) are nuclear organelles that contain factors required for splicing, ribosome biogenesis and transcription. Our previous analysis in living cells showed that CBs are dynamic structures. Here, we show that CB mobility is described by anomalous diffusion and that bodies alternate between association with chromatin and diffusion within the interchromatin space. CB mobility increases after ATP depletion and inhibition of transcription, suggesting that the association of CB and chromatin requires ATP and active transcription. This behaviour is fundamentally different from the ATP-dependent mobility observed for chromatin and suggests that a novel mechanism governs CB, and possibly other, nuclear body dynamics.

The CB was first identified as an accessory of the nucleolus by Ramón y Cajal[1]. In somatic cells, CBs vary in size (0.1–2.0 μm in diameter) and number (0–10), depending on the cell type and the stage of the cell cycle, with higher numbers found in proliferating cells[2–4]. CBs contain a number of factors that are involved in transcription, splicing, small nuclear RNA (snRNA) processing and signalling. These include snRNPs, survival of motor neuron protein (SMN), the U3, U8 and U14 snoRNAs, the U7 snRNA, nucleolar proteins (such as NOPP140 and fibrillarin) and basal transcription factors (such as TFIIF, TFIIH, the TATA binding protein (TBP), PTF-γ and RNA polymerases I and II)[3,5]. These factors may be assembled or processed in CBs before delivery to their sites of action[3]. Newly assembled splicing snRNPs enter the nucleus and accumulate in CBs before concentrating in speckles[6]. CBs also contain p80 coilin, a human auto-antigen used as a marker for CBs. Members of the SMN protein and snRNP complex are not recruited to CBs in knockout mice bearing carboxy-terminal truncations of p80 coilin[7]. In addition, *Xenopus laevis* egg extracts depleted of a coilin homologue fail to target snRNPs to CBs[8]. These data are consistent with the hypothesis that p80 coilin and CBs function in the snRNP transport and maturation pathway.

In living plant and animal cells, CBs are dynamic structures. They move through the nucleoplasm and can join to form larger CBs, or split to produce individual CBs with different protein composition[9–11]. In fixed somatic cells and oocytes, CBs associate with the histone and snRNA genes[12–18]. These associations might reflect a direct tethering of CBs to constituents of specific gene loci. Alternatively, CBs may repeatedly associate with and dissociate from individual loci. The molecular mechanisms that influence CB association with chromatin and the paths CBs take between sites is not known. Finally, a requirement for ATP in the behaviour of CBs has not been established. In this study, we compare the movement of CBs to that of chromatin and examine the effects of inhibiting DNA transcription and removing ATP on CB dynamics.

Results

Interactions of CBs and chromatin. Our previous work identified a striking diversity in the molecular composition, morphology and dynamic behaviour of CBs in cultured HeLa cells expressing a green fluorescent protein (GFP)–coilin fusion protein[10]. Because CBs can be found juxtaposed to gene loci[12,17,19], we analysed the interactions of CBs and chromatin in living cells. The HeLa$^{GFP–coilin}$ cell line[10] was transfected with a plasmid encoding human histone H2B fused to the yellow fluorescent protein (H2B–YFP). This type of fusion has been used previously to produce a functional fluorescent form of histone H2B[20](see Methods).

Time-lapse imaging revealed that CB mobility changes dramatically when it is closely associated with chromatin. A representative example from a HeLa$^{GFP–coilin}$ cell transfected with histone H2B–YFP is shown (Fig. 1). The coloured arrow (Fig. 1a) points to a CB translocating through the nucleoplasm, apparently between masses of chromatin. The positions of the same CB relative to chromatin are represented by the purple dot placed on the histone H2B–YFP images. Initially, the CB barely moves (Fig. 1a; 00:00:20 and 00:22:40) and is surrounded by chromatin. It then departs from this dense chromatin region (Fig. 1a; 00:49:57) and begins to move through the nucleoplasm. After associating briefly with the surface of the nucleolus (Fig. 1a; 01:01:22), the CB moves rapidly (Fig. 1a; 01:28:08–01:54:36) until it comes to rest, again juxtaposed to another block of chromatin (Fig 1a; 02:10:36–02:37:59). In the example shown, and in 40 other nuclei examined, CBs that show little movement were either surrounded by, or in contact with, dense chromatin regions. However, as discussed below, proximity to chromatin does not always slow CB mobility. In addition, the associations observed in Fig. 1 do not necessarily indicate direct binding to chromatin. For clarity, we will refer to these events as association between CBs and chromatin.

To quantify CB mobility, we have used analytical methods derived from single particle tracking (SPT[21]). This approach calculates a diffusion constant (D) from the movements of an object over a range of time intervals. We determined diffusion constants for short time intervals at each point in the time-lapse images for the CB highlighted in Fig. 1a (Fig. 1b; see Methods). The colours of the arrows in Fig. 1a match the colours of the bars in Fig. 1b. The diffusion constant of this CB changes by over 20-fold; it is at its minimum when the CB is associated with chromatin (Fig. 1a, purple and yellow arrows and 1b, purple and yellow bars) and at its maximum when the CB is not closely associated to chromatin (Fig. 1a, red arrows and Fig. 1b, red bars). When the CB associates

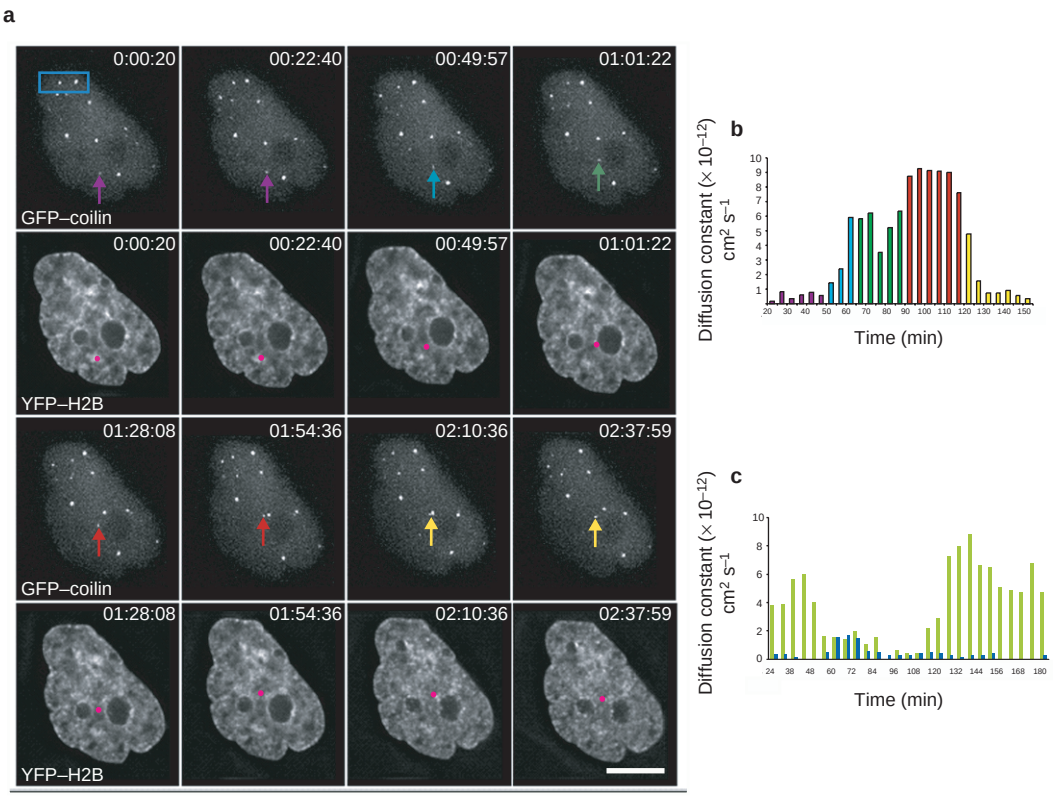

Figure 1 **CB movement and its relation to chromatin.** A plasmid encoding histone H2B–YFP was transfected into HeLa$^{GFP–coilin}$ cells (see Methods). **a**, Optical sections from the time-lapse 3D data set are shown for the GFP–coilin signal (first and third rows) and the H2B–YFP signal (second and fourth rows). Elapsed time is indicated at the top right of each image. The coloured arrow follows a CB at the beginning of data collection as it is associated with chromatin (00:00:20–00:22:40, purple arrow), dissociates and diffuses (00:49:57, blue arrow), then briefly associates with the surface of the nucleolus (01:01:22, green arrow), again dissociates and diffuses (01:28:08–01:54:36, red arrows) and then associates again with chromatin at a new site. In all cases, movement of this CB and all others takes place in the space between dense blocks of chromatin. The colours of the arrows in the coilin images correspond to the times plotted in **b**. Scale bar, 10 μm. **b**, A plot of the short-term diffusion constants of the CB shown in **a**. The coloured bars of the histogram represent the diffusion constant of the CB at each time and correspond to the position of the CB in the nucleus, as indicated by the coloured arrow in **a**. **c**, A histogram showing the short-term diffusion constants of two individual CBs through a time-lapse image from the same nucleus shown in **a** and **b**. The CBs are indicated by the blue box in **a**. The CB that is associated with chromatin (blue bars) has lower mobility than the CB that does not associate with chromatin (green bars). Changes in mobility occur independently of other CBs (**a** and **b**).

with dense chromatin surrounding the nucleolus (Fig. 1a, green arrow), its mobility transiently decreases (Fig. 1b, green bars). This analysis suggests a correlation between CB mobility and association with chromatin. Additionally, our results indicate that single CBs can interact with multiple distinct chromatin loci.

A similar analysis for neighbouring CBs (for example, Fig. 1a, blue box) showed similar changes, but no correlation between diffusion constants of neighbouring CBs (Fig. 1c). Although more sophisticated techniques might identify subtle correlations, our current evidence suggests that CBs may associate or interact with chromatin without regard to the state of neighbouring CBs.

In summary, these results strongly correlate CB mobility with their close association to, and possible interaction with, dense regions of chromatin. Associations with chromatin seem to limit CB mobility. By contrast, dissociation from chromatin allows CBs to migrate within the interchromatin space at much higher rates.

Characteristics of CB mobility. We next analysed the characteristics of CB mobility and interactions with their environment using SPT. Plots of the average change in position for CBs, known as the mean square displacement (MSD), over a range of time intervals (Δt) determine whether particles diffuse randomly (Fig. 2a,d), in the presence of physical constraints (Fig. 2b,e) or external forces (Fig. 2c,f)[21]. We have used this method to determine whether CB mobility is active or passive, and to detect interactions between CBs and their local environment.

The motion of individual CBs from 70 nuclei was assigned to one of the three classes shown in Fig. 2. In this analysis, 31% of CBs seemed to diffuse randomly; in these instances, the MSD showed a linear relationship with time interval (Fig. 2g). The behaviour of another 52% of CBs was consistent with constrained diffusion, in which the MSD reaches a plateau at longer time intervals (Fig. 2h). This might occur either because a CB is trapped within a domain or because it is tethered to another nuclear structure. CBs that diffuse slowly (Fig. 2g) may in fact be constrained, and it is possible that diffusion occurs too slowly to reveal the constraint. Finally, the MSD plots of 17% of CBs showed a positive curvature, consistent with diffusion in the presence of a flow or some other external force (Fig. 2i). Thus, the majority of CBs (83%) behave as if they passively diffuse within a volume that is limited by some form of a constraint or tether. The data shown in Figs 1 and 2 strongly suggest that the CB constraint or tether is chromatin, includes chromatin, or else some factor that is closely associated with chromatin. Indeed, removal of most of the chromatin in HeLa$^{GFP–coilin}$ cells with DNAse I caused a reduction in the number of CBs present in each nucleus. The remaining CBs were always juxtaposed to residual chromatin masses (see Supplementary Information, Fig. S1).

ATP levels and active transcription affect CB dynamics. To study the mechanism of CB mobility, we next depleted ATP levels in HeLa$^{GFP–coilin}$ cells and then determined CB diffusion constants from plots of MSD against Δt. Treatment of cells with the respiration

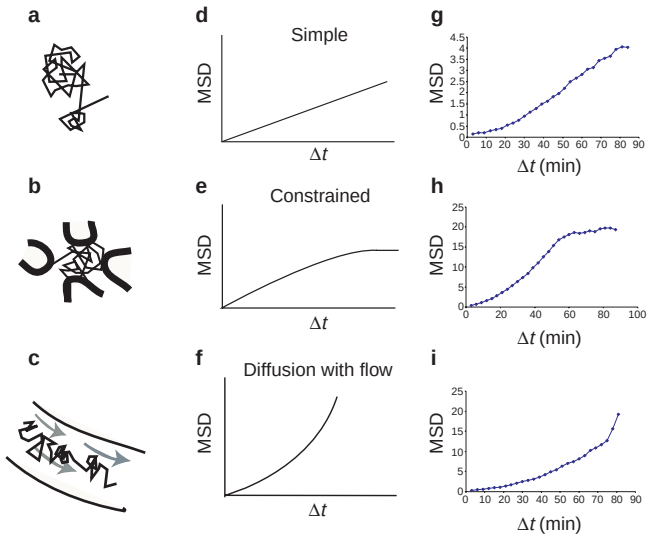

Figure 2 **Different types of CB movement in live HeLa$^{GFP–coilin}$ cells.** **a**–**c**, Diagrams representing theoretical trajectories of particles undergoing random diffusion (**a**), constrained diffusion caused by interactions of the diffusing particle with other mobile or immobile barriers (**b**) and diffusion in the presence of flow or other exogenous force (**c**). **d**–**f**, Theoretical plots of MSD as a function of time interval (Δt). The MSD of a freely diffusing particle has a linear relationship with Δt (**d**; that is, the longer the time interval, the further the particle has moved). Therefore, a monotonic increase of MSD with increasing Δt suggests simple diffusion. If a barrier or tether limits the distance a particle can move, its diffusion is constrained and the MSD initially increases in a linear relationship with Δt. It then plateaus and increases no further, even with infinite Δt (**e**). As Δt increases, the MSD becomes independent of Δt and the plot reaches a plateau. This assumes that the constraint remains constant throughout the trajectory and that the length of data collection is sufficient to reveal constraint. If the particle diffuses in the presence of a flow, as a result of other particles or another exogenous force, the MSD increases disproportionately with Δt. An upwardly curving parabolic curve is indicative of diffusion with flow or directed motility (**f**). In all cases, the initial slope of these plots is directly proportional to the diffusion constant of the particle (see Methods)[21]. The diffusion constant, as revealed in the initial slope of the MSD plot, can be large or small, independently of the effect of a constraint. **g**–**i**, Representative plots of MSD versus Δt of individual CBs obtained by SPT analysis in live HeLa$^{GFP–coilin}$ cells. Different types of movement for individual CBs were observed and can be categorized as simple diffusion (**g**), constrained diffusion (**h**) or diffusion with flow (**i**).

inhibitor sodium azide, either alone or in conjunction with the glycolysis inhibitor 2-deoxyglucose, caused no detectable change in the number of CBs or their GFP–coilin content (data not shown). Surprisingly, depletion of cellular ATP levels caused a significant increase in the mobility of CBs. Time-lapse images of GFP–coilin and histone H2B–YFP in control cells (Fig. 3a, left) and ATP-depleted cells (Fig. 3a, right; see also Supplementary Information movies) are shown. In control cells, most CBs were found closely juxtaposed to chromatin (Fig 3a, left; arrowheads). By contrast, depletion of ATP (Fig. 3a, right) caused a marked change in the degree and nature of CB mobility. CBs explored larger domains, apparently bounded by dense chromatin regions. CBs contacted chromatin, but did not remain stably associated, as in control cells (Fig. 3a, right; arrowheads). Plots of CB trajectories through both time-lapse sequences show that the volume explored by all CBs is higher after ATP depletion (Fig. 3b). Nonetheless, the diffusion of CBs after ATP depletion is limited by dense chromatin masses. Within the resolution limits of our data, we did not observe any changes in chromatin structure during ATP depletion.

To see if this difference in mobility was common to most CBs, we calculated diffusion constants from MSD plots from 351 CBs in con-

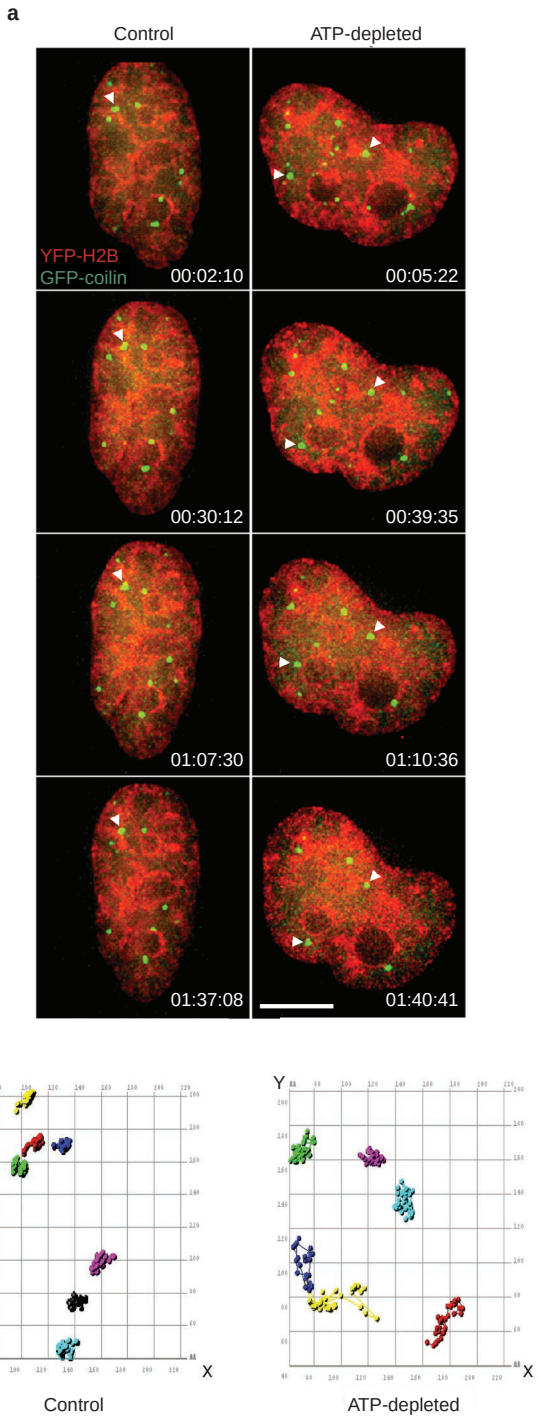

Figure 3 **The mobility of CBs within the interchromatin space is dependent on ATP.** **a**, H2B–YFP was transfected into HeLa$^{GFP–coilin}$ cells (see Methods). Four frames (maximum intensity projections of deconvolved data sets) from 3D time lapse data sets are shown for GFP–coilin (green) and the H2B–YFP (red) in a control nucleus (left) and a nucleus after ATP depletion (right). CBs in the energy-depleted nuclei move with much higher diffusion constants within the interchromatin space. Characteristic movements of CBs in either control or energy-depleted nuclei can be followed (white arrowheads). Scale bar, 10 μm. **b**, Trajectories of individual CBs from the cells in **a**. Individual CB trajectories are colour coded and all data collected during a 1-h recording (images recorded every 3 min) is shown. After ATP depletion, the majority of CBs do not remain associated with dense chromatin regions, but instead explore a much larger volume of the nucleus, suggesting that ATP is needed for the tethering of CBs.

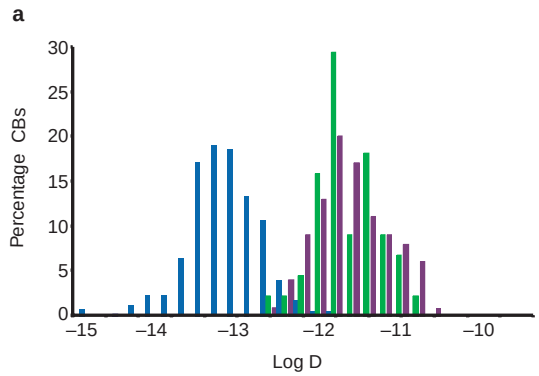

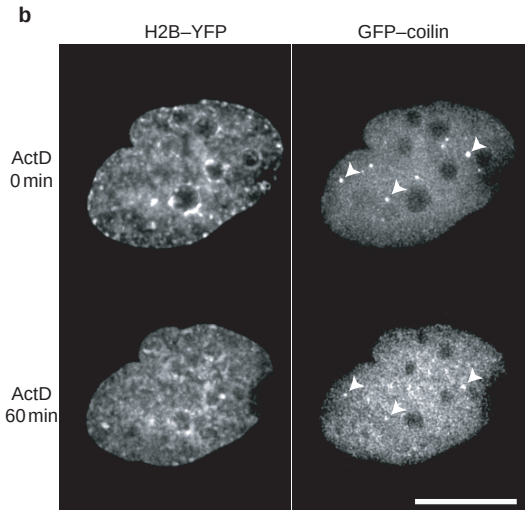

Figure 4 **ATP depletion and transcriptional inhibition affect the mobility of CBs. a**, Distributions of log D (diffusion constants) from SPT measurements of control CBs and CBs after energy depletion and inhibition of transcription by ActD. A histogram of the distribution of log D plotted against the percentage of CBs is shown. D represents diffusion constants of CBs in control medium (blue bars), in medium supplemented with 10 mM sodium azide (purple bars) and in medium supplemented with 10 μg ml^{-1} ActD (green bars). Note the shift of log D distribution between control CBs and CBs after energy depletion and inhibition of transcription. **b**, The effects of ActD on chromatin organization in living cells. A plasmid encoding histone H2B–YFP was transfected into HeLa$^{GFP–coilin}$ cells (see Methods). Maximum intensity projections from 3D sets are shown. The histone H2B–YFP signal (left) and the GFP–coilin signal (right) are shown in a living cell before and after incubation in ActD for 1 h, with no other data acquisition in the intervening period. Arrowheads indicate the same CBs before and after ActD treatment. After inhibition of transcription, both dense heterochromatic and euchromatic regions seem less well defined and organized. Scale bar, 10 μm.

trol cells and 150 CBs in ATP-depleted cells. The distribution of CB diffusion constants in ATP-depleted cells shifts by over an order of magnitude when compared to control cells (Fig. 4a, blue and pink bars), showing quantitatively that the mobility of most CBs is affected by cellular ATP levels. The simplest interpretation of these data is that CBs can be tethered to chromatin or a factor closely associated with chromatin, and that this tethering is ATP-dependent.

Because CBs contain many factors involved in transcription and mRNA splicing, the ATP requirement for CB release from chromatin may involve active transcription or splicing. We next examined whether transcriptional activity affected CB mobility by treating HeLa$^{GFP–coilin}$ cells with the transcriptional inhibitor actinomycin D

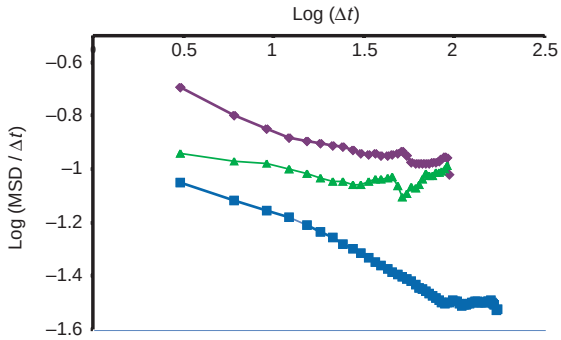

Figure 5 **Anomalous diffusion of CBs requires ongoing transcription and energy.** MSDs of 150 CBs were plotted as log (MSD/Δ*t*) versus log (Δ*t*) (blue line). Anomalous diffusion is indicated by a straight line with an initial negative slope of $(2/d_w - 1)$; when Δ*t* is large, relative to the time for changes in CB association, diffusion appears normal and the plot changes to a horizontal line. The intersection of the diagonal and horizontal parts of the plot defines the crossover time, t_{cr}. The larger the slope in the anomalous region, the larger the anomalous diffusion exponent d_w. Anomalous diffusion can be caused by obstacles or binding sites that affect the diffusion of a particle. After ActD treatment (green line; mean of MSD of 50 CBs) or energy depletion (purple line, mean of MSD of 102 CBs) the interactions with binding sites decreases, as indicated by the decrease in the slope of both lines. Diffusion of the CBs becomes normal, as indicated by the horizontal line, and the crossover time between anomalous and normal diffusion decreases. Both energy and ongoing transcription are required to maintain the binding sites and obstacles with which CBs interact.

(ActD). Treatment with ActD caused an increase in the distribution of CB diffusion constants (Fig. 4a, green bars). The shift in distribution was similar to that observed during ATP depletion. Both in the control and in the treated CBs, the distribution of log D remains two orders of magnitude wide, emphasizing the heterogeneity of CB dynamics. This heterogeneity is maintained after ATP depletion, but the distribution shifts to larger log D. This may reflect the fact that similar pathways are inhibited by both treatments. This result agrees with previous suggestions that CBs only associate with transcriptionally competent snRNA loci[22,23] and suggests that CB association with chromatin may accompany active transcription.

As CB mobility in untreated cells seems to be restricted by interactions with chromatin (Figs 1 and 2), we examined the structure of chromatin in the presence of ActD. The localization of histone H2B–YFP and GFP–coilin in the same cell is shown, before and after a 1-h incubation with ActD (Fig. 4b). This treatment caused the loss of dense chromatin regions and higher-order structure in euchromatin (Fig. 4b). These results suggest that CB mobility increases in ActD-treated cells either because chromatin structure is disrupted or because transcription is inhibited.

To further characterize the role of ATP in CB dynamics, we inhibited ATP-dependent actin polymerization with latrunculin A[24]. This did not alter CB mobility (Fig. 6a), despite causing significant cell rounding, retraction from the substrate and loss of cytoplasmic F-actin (data not shown). We conclude that F-actin probably does not directly mediate CB dynamics and most likely is not linked to the dependence of CB dynamics on ATP levels.

Diffusion of CBs is anomalous. Our data suggest that CBs may physically interact with other nuclear components, most likely with chromatin, and that these interactions can change over time (Fig. 1). This heterogeneity of physical states complicates the statistical analyses (Fig. 2) and suggests that treatment of CBs as a single population might obscure differences occurring at different time points in a single CB or between different CBs. A model for this type of interaction is provided by previous analyses of molecular receptors diffusing within the plasma membrane and physically interacting with the cytoskeleton or specialized regions of the membrane. Tracking the motions of these receptors identified an anomalous

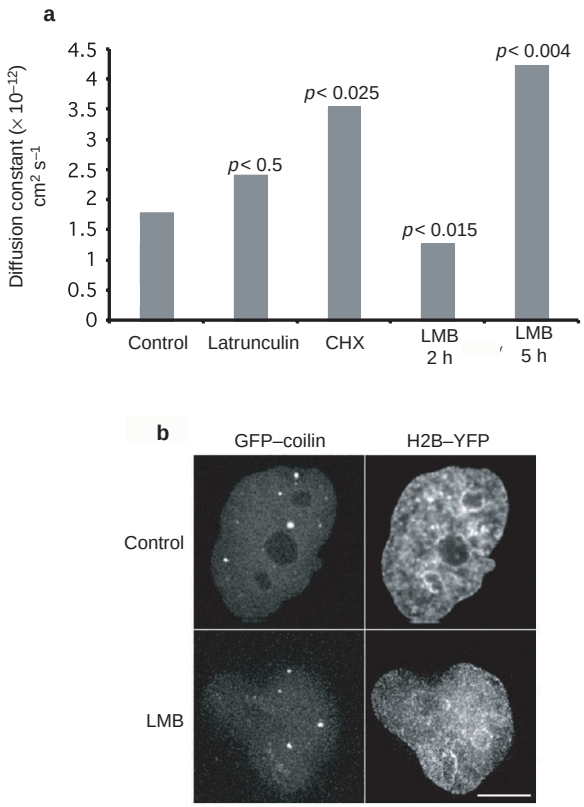

Figure 6 **CB mobility is dependent on protein synthesis and nuclear export.** **a**, HeLa$^{GFP–coilin}$ cells were treated with various inhibitors and CB diffusion constants were determined by SPT (see Methods). The histogram shows the mean of diffusion constants from populations of CBs under each condition. Statistically significant differences were detected by a two-tailed *t* test and are indicated by the value of *p* for each measurement. *p* values < 0.05 are indicative of averages over two statistically different populations. Inhibition of actin polymerization with latrunculin does not significantly change the mean CB diffusion constant. CBs are significantly more mobile after treatment with CHX, suggesting that protein synthesis is required for the association of CBs to chromatin. A similar result was observed when cells were incubated with LMB for 5 h. Shorter incubations in LMB identified a significant decrease in CB mobility, suggesting that Crm1 may be involved in regulating CB mobility. **b**, LMB treatment affects chromatin structure in HeLa$^{GFP–coilin}$ cells. A plasmid containing H2B–YFP was transfected into HeLa$^{GFP–coilin}$ cells (see Methods). Maximum intensity projections from time-lapse 3D data sets are shown. The distribution of GFP–coilin (left) and H2B–YFP (right) is shown in both the control nucleus and the LMB-treated nucleus (30 nM for 5 h). At this time, coilin has just started to appear in the nucleolus, where it is concentrated at later times during LMB treatment[32]. Note the disruption of chromatin structure and the reduction of the chromatin condensed regions. No clear distinction now exists between condensed and less condensed chromatin regions and the interchromatin space.

Table 1 Changes in the anomalous diffusion of CBs.

	Anomalous diffusion exponent (d_w)
Control	2.99
Cycloheximide	2.85
Leptomycin B 2 h	3.12
Leptomycin B 5 h	2.77
Sodium azide	2.55
Actinomycin D	2.21

The anomalous diffusion exponent (d_w) was calculated from the slope of the log (MSD/Δ*t*) versus log (Δ*t*) plots based on trajectories of CBs from time-lapse images of HeLa$^{GFP–coilin}$ cells. The slope was determined using a least-squares regression covering the linear part of the plots. Treatments are described in the Methods. Number of CBs used in each plot: control, 150; CHX, 74; LMB 2 h, 83; LMB 5 h, 77; sodium azide, 102; ActD, 54.

form of diffusion as a result of these interactions[25–27]. Anomalous diffusion occurs when a particle switches between a freely diffusing state and a bound or constrained state. Instead of a linear relationship between MSD and Δ*t* that is found in normal diffusion (Fig. 2), anomalous diffusion is characterized by an exponential relationship[28] (see Methods).

We tested whether CB dynamics fit a model of anomalous diffusion by plotting the log (MSD/Δ*t*) versus log(Δ*t*). For normal diffusion, this plot gives a horizontal line with slope = 0. Anomalous diffusion, where MSD is related to Δ*t* by an exponential, gives a line with negative slope equal to 2 divided by $d_w - 1$ (d_w is the anomalous diffusion exponent; see Methods)[28,29]. A plot for CBs in living HeLa$^{GFP–coilin}$ cells is shown (Fig. 5, blue line). The negative slope clearly indicates that CBs diffuse anomalously. Furthermore, at longer time intervals this line becomes horizontal and diffusion is effectively normal. This transition is defined as the crossover time, t_{cr} and is a measure of the density and affinity of binding sites[28]. This statistical analysis demonstrates that CB diffusion is anomalous and that CBs can switch between states where they are constrained or tethered and where they diffuse freely.

We also used this approach to analyse the effects of ATP depletion and inhibition of transcription by ActD on CB mobility. Depletion of ATP (Fig. 5, purple line) makes the log (MSD/Δ*t*) plot less steep and decreases d_w (Table 1), indicating a shift in the mode of CB diffusion from anomalous to normal. This result, along with those shown in Figs 3 and 4, suggests that ATP depletion causes a decrease in the association of CBs and chromatin through either a loss of binding sites or a decrease in the binding energy between CBs and chromatin.

Inhibition of transcription with ActD decreased the slope of the log (MSD/Δ*t*) plot (Fig. 5, green line) and d_w (Table 1), again indicating a change in the mode of CB diffusion from anomalous to normal. We conclude that CBs shift between chromatin-associated and non-associated states in a manner that is dependent on ATP and/or active transcription.

The association of CBs and chromatin is unstable. We next examined the effect of inhibiting protein synthesis on CB dynamics. When HeLa$^{GFP–coilin}$ cells are exposed to cycloheximide (CHX), CB diffusion constants increased (Fig. 6a) and d_w decreased (Table 1), demonstrating that the factor(s) required for CB association with chromatin are either no longer present, or else inactive. As histones are not known to be rapidly degraded, this result strongly suggests that at least one non-histone protein mediates the association of CBs and chromatin.

Leptomycin B (LMB) inhibits the export of certain proteins and RNA from the nucleus by binding to Crm1 and preventing its association with export substrates[30,31]. Short incubations in LMB increase the association of CBs with snRNA genes[23]. Treatment of HeLa$^{GFP–coilin}$ cells with LMB for 2 h decreased the mean CB diffusion constant (Fig. 6a) and increased the degree of anomalous diffusion, as indicated by d_w (Table 1). By contrast, treatment with LMB for 5 h caused an increase in the mean CB diffusion constant (Fig. 6a), a decrease in d_w (Table 1) and disrupted the association between CBs and snRNA genes[23]. Thus, changes in mobility and anomalous diffusion explain the differences in the association of CBs and gene loci previously observed in LMB-treated cells. The complex effects that result from LMB treatment may reflect the downstream consequences of blocking U snRNA transport, a direct effect on Crm1, or possibly the depletion of a specific factor required for association of CBs and chromatin through inhibition of RNA export[23,32]. Attempts to examine CB dynamics after longer LMB incubation were not possible because of significant redistribution of p80 coilin[32].

LMB Affects Chromatin Structure. Crm1 was originally identified as a gene that is necessary for maintaining chromosome structure in *Schizosaccharomyces pombe*[33]. To determine if the effects of LMB on CB mobility might be also caused by changes in mammalian chromatin, we examined living HeLa$^{GFP–coilin}$ cells expressing histone H2B–YFP after incubation in LMB. Chromatin in living HeLa$^{GFP–coilin}$ cells incubated with LMB for 5 h seemed much less condensed than in controls, suggesting that some aspect of higher-order chromatin structure was disrupted after LMB treatment (Fig. 6b). Similar results were observed with cells expressing YFP–HP1γ, a marker for heterochromatin[34] (data not shown). Changes in higher order chromatin structure in LMB-treated cells may contribute to loss of association of CBs with specific gene loci. By contrast, LMB treatment for 2 h, which decreased CB mobility (Fig. 6a), caused no detectable changes in chromatin structure (data not shown).

Discussion

Using dual-wavelength imaging of living cells and statistical image analysis techniques, we show for the first time that CBs exist in at least two states: closely associated with chromatin or freely diffusing in spaces between chromatin domains. Most movements of CBs are consistent with passive diffusion, although the motion of a subpopulation (17%) may be influenced by an external force. Our results demonstrate a link between nuclear body movements and ATP, provide evidence that the association of CBs with chromatin may be a major regulator of CB dynamics and suggest that this interaction is dependent on transcription.

Passive diffusion is the dominant mode of CB movement, although 17% of CBs seem to move in the presence of an exogenous force (Fig. 2). This is a significant minority, and although we cannot exclude a role for an ATP-dependent motor in these events, it is also possible that the diffusion of CBs through spaces between chromatin masses guides the movement of this CB subpopulation. Moreover, when ATP is depleted, the distribution of CB diffusion constants shifts (Fig. 4a), suggesting that the effect of ATP hydrolysis is common to at least the majority of CBs. Our results are therefore most consistent with a role for ATP, either directly or indirectly, in the association of CBs with chromatin or chromatin-associated factor(s). In many time-lapse images, including the example shown in Fig. 1a, a CB that is initially surrounded by chromatin is released, coincident with a local change in the chromatin. Thus, the nature of the ATP requirement for CB association may take many forms, including a mechanochemical motor or a chromatin remodelling activity.

A critical finding in our results is the switching of individual CBs between chromatin-associated and freely diffusing states in living cells. This explains the statistical variation observed in previous analyses of CB–chromatin association in fixed cells[12] and is consistent with suggestions that CBs function as sites of transit or maturation of splicing and transcription factors[3,5,6]. A corollary of this model is the possibility that CBs assist the assembly and delivery of large macromolecular complexes to transcriptionally active sites. This function might not be absolutely essential: transcription or splicing complexes could assemble on their own within the nucleoplasm, based on random diffusion, but concentration of these factors into a specific site, such as the CB, might accelerate or improve the efficiency of their assembly or modification. This model predicts that defective CBs might cause a growth phenotype. Indeed, mice bearing deletions of p80 coilin show reduced viability and contain residual CBs that fail to recruit known CB components, such as snRNPs and the SMN complex[7].

There is abundant evidence to indicate that the location of nuclear organelles can correlate with their function. Individual chromosomes occupy distinct territories[35] and their position relative to the nuclear envelope is correlated with the density of genes on each chromosome[36]. Individual genetic loci move away from the repressive environment of centric heterochromatin after transcriptional activation[37–39]. Finally, individual loci migrate towards the interior of the nucleus before being replicated and return to a peripheral location afterwards[40]. In *Saccharomyces cerevisiae*, *Drosophila melanogaster* and human cells, the diffusion of chromatin is generally constrained, either by tethers or boundaries[41–43]. Thus, a shift in chromatin location might require the release of a mobility constraint before diffusion to a new location[44], where the constraint or tethering might be re-established. These transitions are similar to those observed here for the anomalous diffusion of CBs, so chromatin dynamics may also be characterized by anomalous diffusion. Recent *in vivo* analysis suggests that this is in fact the case[45]. The mechanics of releasing a gene locus for diffusion may be more complex than for a CB, as the locus will always be attached to the remaining length of a chromosome. Interestingly, ATP depletion in *S. cerevisiae* decreases the mobility of chromatin[41,46], so CB dynamics differ fundamentally from chromatin. Moreover, analysis of PML body movement[47] identified rates of movement that were significantly faster than we previously reported for CBs[10] and demonstrated that movement of some PML bodies was inhibited by ATP depletion. The size of PMLs vary, but they are approximately the same size or larger than CBs, suggesting that the behaviour of each these structures depends on a complex mix of molecular and physical characteristics, and not simply their size (see Supplementary Information, Section II).

Whether applied to CB or chromatin dynamics, an appealing aspect of an anomalous diffusion model is its emphasis on the interaction of an object with its local environment. There is increasing evidence that the nucleus is divided into a series of functionally distinct compartments, so migration of macromolecules, complexes and nuclear bodies between nuclear compartments[44,48,49] is likely to be an important mechanism in the regulation of transcription and replication. Techniques such as SPT, which can address the conditions in subdomains of the nucleus, should be especially powerful in dissecting these processes. Because nucleoplasmic macromolecules also seem to switch between bound and freely moving states[48,50], an examination of the dynamics of individual nuclear molecules may identify how these factors find their target sites. The future application of this technique to cells with separately labelled nuclear bodies and genetic loci will allow direct analysis of the consequences of CB association with chromatin. □

Methods

Plasmids

The histone H2B full-length cDNA was amplified from the Human HeLa Marathon-Ready cDNA library (Clontech, Hampshire, UK) using the 5′-primer H2BYFP-F1, which contains a *Kpn*I restriction site (in bold) (5′- CG**GGTACC**GCCACCATGCCAGAGCCAGCGAAGTCTGCT-3′) and a 3′-primer H2BYFP-R1, which contains a *Bam*H1 restriction site (in bold) (3′-CG**GGATCC**TTAGCGCTGGTG-TACTTGGTGAC-5′). The resulting PCR fragment was digested with *Kpn*I and *Bam*H1 and cloned into the pEYFPN1 vector (Clontech) to give rise to the pEYFP-H2B plasmid. The *Kpn*I–YFPH2B–*Bam*HI internal portion of the plasmid was sequenced and contained the expected Histone H2B sequence. The YFP–HP1γ plasmid was a kind gift of A. Fox (University of Dundee, UK).

Cell culture, transfection and imaging

HeLa$^{GFP–coilin}$ cells were grown and imaged as previously described[10]. The HeLa$^{GFP–coilin}$ cell line contains a fusion of GFP with the CB marker p80 coilin, under the control of the Tet-off inducible promoter[10]. Transfections were performed using the Effectene transfection reagent (Qiagen, West Sussex, UK) according to the manufacturer's protocol. HeLa$^{GFP–coilin}$ cells were transfected four to five days before imaging to allow replication-dependent incorporation of transfected proteins. No change in growth rates, mitotic index or number of apoptotic cells was observed. Five days after transfection, histone H2B–YFP was localized to chromatin and concentrated in heterochromatin at the nuclear periphery and around the nucleolus (Fig. 1a). Histone H2B–YFP also colocalized with anti-histone and DAPI staining (data not shown). Previously, we identified multiple populations of CBs in HeLa cells[10]. In this report, we refer to all of these simply as CBs. Imaging was performed as previously described[10], using a DeltaVision Restoration Microscope (Applied Precision, Issaquah, WA).

Drug treatments

Latrunculin A: to assay the requirement for F-actin on CB dynamics, HeLa$^{GFP–coilin}$ cells were imaged as normal for 30 min, then perfused with medium containing 5 μM latrunculin A. Time-lapse imaging was resumed 20 min later. Imaging of cells for longer than 1 h in the presence of latrunculin A was difficult because of rounding of the cells and movement of nuclei out of the plane of focus.

ATP Depletion: 10 mM sodium azide, either alone or in combination with 50 mM 2-deoxyglucose (2-DG; Sigma, Dorset, UK), was added to the medium 30–60 min before imaging for 1.5 h. This treatment prevented mitochondrial staining with MitoTracker Red CMH2Xros, consistent with depolarization

of the mitochondrial membrane (data not shown). The MitoTracker Red CMH2X Ros probe is oxidized to its fluorescent form only when it enters the mitochondrion of an actively respiring cell, and hence only stains polarized mitochondrial membranes. Removal of sodium azide and 2-DG restored mitochondrial staining and produced a decrease in CB diffusion constants, but did not alter cell viability. Control experiments showed that the ATP depletion protocol significantly decreased MitoTracker fluorescence, indicating a loss of mitochondrial membrane polarization and inhibition of mitochondrial ATP synthesis.

Actinomycin D: ActD (Sigma) was added to cells at a concentration of 10 μg ml^{-1}. Data collection started 15–20 min after addition of ActD and continued for 1.5 h.

Leptomycin B: LMB (Sigma) was added at a concentration of 30 nM for 45–90 min before imaging. Imaging took place for 2.5 h. Alternatively, LMB was added for 5 h before time-lapse imaging for another 2.5 h. Imaging was carried out in the presence of 30 nM LMB.

Cycloheximide: CHX (Sigma) was added to the medium at a concentration of 100 μg ml^{-1} for 1 h before imaging. The same amount of CHX was included in the medium during imaging.

Cells were not synchronized for any of the treatments, but maximum effort was taken to ensure that all experimental setups were the same, including cell confluency, plating date and growth rate.

Statistical methods for the qualitative analysis of motion

To assess the statistical significance of differences in mean CB diffusion constants under different treatments, we determined whether variances were equal or unequal using an F-max test. The appropriate *t*-test for equal or unequal variances was then performed. The alpha level for all tests was set to 0.05.

Calculation of diffusion constants

We used a segmentation algorithm based on a statistically calculated threshold to identify and track three-dimensional trajectories of CBs in time-lapse images[10]. Our analysis of these trajectories was based on previous studies of diffusion in the plasma membrane and the nucleus[21,41]. By denoting a time interval as Δt and the 3D position of a CB at any time t as $d(t)$, we calculated the MSD for each CB for all Δt in a time-lapse data set: $MSD(\Delta t) = [d(t) - d(t + \Delta t)]^2$.

A plot of MSD against Δt (Fig. 2) demonstrates whether a CB diffuses normally, under a constraint, or in the presence of an exogenous flow or other force[21]. The initial slope of this plot is equivalent to six times the diffusion constant. Calculating the MSD across all time intervals reduces the noise in the calculation from experimental trajectories[21,41,51,52]. However, we were able to monitor changes in the diffusion constant through a time-lapse data set by calculating MSDs and the diffusion constant across a short time window (10–15 min), shifting the time window and then recalculating the diffusion constant. These short-term diffusion constants use many fewer measurements and are therefore less accurate than those calculated across a whole trajectory. Nonetheless, they identify changes in the diffusion constant (Fig. 1b) that are averaged out by analysis across a whole trajectory.

Analysis of anomalous diffusion

In unobstructed diffusion, the MSD of the diffusing particle is proportional to Δt. The presence of obstacles to free diffusion or binding sites results in anomalous diffusion. In this case, there is no longer a linear relationship between MSD and Δt. Instead, MSD is proportional to a fractional power of time less than one: $MSD \sim t^{2/d_w}$, where d_w is the anomalous diffusion exponent. Values of $d_w > 2$ indicate anomalous diffusion[26,28,29].

To visualize anomalous diffusion, we plotted the MSD results on a logarithmic scale as log (MSD/Δt) versus log(Δt), (Fig. 5)[29]. If diffusion is anomalous, then this plot generates a straight line with a negative slope of $2/d_w - 1$. Normal diffusion gives a horizontal line with a slope of 0. Typically, short time intervals reveal a negative slope and anomalous behaviour, but at longer time intervals, where the effect of transient binding events is masked, the plot switches to a horizontal line[28]. The position of the transition from anomalous to normal diffusion, or the crossover time (t_c), is a measure of the number of obstacles and affinity of binding sites. As the number of sites or the binding energy decrease, d_w and t_c decrease because the probability of interaction decreases.

RECEIVED 18 DECEMBER 2001; REVISED 30 APRIL 2002; ACCEPTED 15 MAY 2002; PUBLISHED 17 JUNE 2002.

1. Ramón y Cajal, S. Un sencillo metodo de coloracíon selectiva del reticulo protoplasmico. *Trab. Lab. Invest. Biol. (Madrid)* **2,** 129–221 (1903).
2. Brasch, K. & Ochs, R. L. Nuclear bodies (NBs): a newly 'rediscovered' organelle. *Exp. Cell Res.* **202,** 211–223 (1992).
3. Gall, J. G. Cajal bodies: the first 100 years. *Annu. Rev. Cell Dev. Biol.* **16,** 273–300 (2000).
4. Andrade, L. E., Tan, E. M. & Chan, E. K. Immunocytochemical analysis of the coiled body in the cell cycle and during cell proliferation. *Proc. Natl Acad. Sci. USA* **90,** 1947–1951 (1993).
5. Matera, A. G. Nuclear bodies: multifaceted subdomains of the interchromatin space. *Trends Cell Biol.* **9,** 302–309 (1999).
6. Sleeman, J. E. & Lamond, A. I. Newly assembled snRNPs associate with coiled bodies before speckles, suggesting a nuclear snRNP maturation pathway. *Curr. Biol.* **9,** 1065–1074 (1999).
7. Tucker, K. E. *et al.* Residual Cajal bodies in *coilin* knockout mice fail to recruit Sm snRNPs and SMN, the spinal muscular atrophy gene product. *J. Cell Biol.* **154,** 293–307 (2001).
8. Bauer, D. W. & Gall, J. G. Coiled bodies without coilin. *Mol. Biol. Cell* **8,** 73–82 (1997).
9. Boudonck, K., Dolan, L. & Shaw, P. J. The movement of coiled bodies visualized in living plant cells by the green fluorescent protein. *Mol. Biol. Cell* **10,** 2297–2307 (1999).
10. Platani, M., Goldberg, I., Swedlow, J. R. & Lamond, A. I. *In vivo* analysis of Cajal body movement, separation and joining in live human cells. *J. Cell. Biol.* **151,** 1561–1574 (2000).
11. Snaar, S., Wiesmeijer, K., Jochemsen, A. G., Tanke, H. J. & Dirks, R. W. Mutational analysis of fibrillarin and its mobility in living human cells. *J. Cell Biol.* **151,** 653–662 (2000).
12. Frey, M. R. & Matera, A. G. Coiled bodies contain U7 small nuclear RNA and associate with specific DNA sequences in interphase human cells. *Proc. Natl Acad. Sci. USA* **92,** 5915–5919 (1995).
13. Gall, J. G., Tsvetkov, A., Wu, Z. & Murphy, C. Is the sphere organelle/coiled body a universal nuclear component? *Dev. Genet.* **16,** 25–35 (1995).
14. Wu, C. H. & Gall, J. G. U7 small nuclear RNA in C snurposomes of the *Xenopus* germinal vesicle. *Proc. Natl Acad. Sci. USA* **90,** 6257–6259 (1993).
15. Gao, L., Frey, M. R. & Matera, A. G. Human genes encoding U3 snRNA associate with coiled bodies in interphase cells and are clustered on chromosome 17p11.2 in a complex inverted repeat structure. *Nucleic Acids Res.* **25,** 4740–4747 (1997).
16. Smith, K. P., Carter, K. C., Johnson, C. V. & Lawrence, J. B. U2 and U1 snRNA gene loci associate with coiled bodies. *J. Cell Biochem.* **59,** 473–485 (1995).
17. Jacobs, E. Y. *et al.* Coiled bodies preferentially associate with U4, U11, and U12 small nuclear RNA genes in interphase HeLa cells but not with U6 and U7 genes. *Mol. Biol. Cell* **10,** 1653–1663 (1999).
18. Shopland, L. S. *et al.* Replication-dependent histone gene expression is related to Cajal body (CB) association but does not require sustained CB contact. *Mol. Biol. Cell* **12,** 565–576 (2001).
19. Callan, H. G., Gall, J. G. & Murphy, C. Histone genes are located at the sphere loci of *Xenopus* lampbrush chromosomes. *Chromosoma* **101,** 245–251 (1991).
20. Kanda, T., Sullivan, K. F. & Wahl, G. M. Histone–GFP fusion protein enables sensitive analysis of chromosome dynamics in living mammalian cells. *Curr. Biol.* **8,** 377–385 (1998).
21. Qian, H., Sheetz, M. P. & Elson, E. L. Single particle tracking. Analysis of diffusion and flow in two-dimensional systems. *Biophys. J.* **60,** 910–921 (1991).
22. Frey, M. R., Bailey, A. D., Weiner, A. M. & Matera, A. G. Association of snRNA genes with coiled bodies is mediated by nascent snRNA transcripts. *Curr. Biol.* **9,** 126–135 (1999).
23. Frey, M. R. & Matera, A. G. RNA-mediated interaction of Cajal bodies and U2 snRNA genes. *J. Cell Biol.* **154,** 499–509 (2001).
24. Morton, W. M., Ayscough, K. R. & McLaughlin, P. J. Latrunculin alters the actin-monomer subunit interface to prevent polymerization. *Nature Cell Biol.* **2,** 376–378 (2000).
25. Smith, P. R., Morrison, I. E., Wilson, K. M., Fernandez, N. & Cherry, R. J. Anomalous diffusion of major histocompatibility complex class I molecules on HeLa cells determined by single particle tracking. *Biophys J.* **76,** 3331–3344 (1999).
26. Feder, T. J., Brust-Mascher, I., Slattery, J. P., Baird, B. & Webb, W. W. Constrained diffusion or immobile fraction on cell surfaces: a new interpretation. *Biophys J.* **70,** 2767–2773 (1996).
27. Simson, R. *et al.* Structural mosaicism on the submicron scale in the plasma membrane. *Biophys J.* **74,** 297–308 (1998).
28. Saxton, M. J. Anomalous diffusion due to binding: a Monte Carlo study. *Biophys J.* **70,** 1250–1262 (1996).
29. Saxton, M. J. Anomalous diffusion due to obstacles: a Monte Carlo study. *Biophys J.* **66,** 394–401 (1994).
30. Fornerod, M., Ohno, M., Yoshida, M. & Mattaj, I. W. CRM1 is an export receptor for leucine-rich nuclear export signals. *Cell* **90,** 1051–1060 (1997).
31. Cullen, B. R. Nuclear RNA export pathways. *Mol. Cell Biol.* **20,** 4181–4187 (2000).
32. Carvalho, T. *et al.* The spinal muscular atrophy disease gene product, SMN: A link between snRNP biogenesis and the Cajal (coiled) body. *J. Cell Biol.* **147,** 715–728 (1999).
33. Adachi, Y. & Yanagida, M. Higher order chromosome structure is affected by cold-sensitive mutations in a *Schizosaccharomyces pombe* gene crm1+ which encodes a 115-kD protein preferentially localized in the nucleus and its periphery. *J. Cell Biol.* **108,** 1195–1207 (1989).
34. Eissenberg, J. C. & Elgin, S. C. The HP1 protein family: getting a grip on chromatin. *Curr. Opin. Genet. Dev.* **10,** 204–210 (2000).
35. Schardin, M., Cremer, T., Hager, H. D. & Lang, M. Specific staining of human chromosomes in Chinese hamster x man hybrid cell lines demonstrates interphase chromosome territories. *Human Genet.* **71,** 281–287 (1985).
36. Croft, J. A. *et al.* Differences in the localization and morphology of chromosomes in the human nucleus. *J. Cell Biol.* **145,** 1119–1131 (1999).
37. Francastel, C., Walters, M. C., Groudine, M. & Martin, D. I. A functional enhancer suppresses silencing of a transgene and prevents its localization close to centrometric heterochromatin. *Cell* **99,** 259–269 (1999).
38. Brown, K. E., Baxter, J., Graf, D., Merkenschlager, M. & Fisher, A. G. Dynamic repositioning of genes in the nucleus of lymphocytes preparing for cell division. *Mol. Cell* **3,** 207–217 (1999).
39. Lundgren, M. *et al.* Transcription factor dosage affects changes in higher order chromatin structure associated with activation of a heterochromatic gene. *Cell* **103,** 733–743 (2000).
40. Tumbar, T. & Belmont, A. S. Interphase movements of a DNA chromosome region modulated by VP16 transcriptional activator. *Nature Cell Biol.* **3,** 134–139 (2001).
41. Marshall, W. F. *et al.* Interphase chromosomes undergo constrained diffusional motion in living cells. *Curr. Biol.* **7,** 930–939 (1997).
42. Bornfleth, H., Edelmann, P., Zink, D., Cremer, T. & Cremer, C. Quantitative motion analysis of subchromosomal foci in living cells using four-dimensional microscopy. *Biophys J.* **77,** 2871–2886 (1999).
43. Marshall, W. F., Dernburg, A. F., Harmon, B., Agard, D. A. & Sedat, J. W. Specific interactions of chromatin with the nuclear envelope: positional determination within the nucleus in *Drosophila melanogaster*. *Mol. Biol. Cell* **7,** 825–842 (1996).
44. Swedlow, J. R. & Lamond, A. I. Nuclear Dynamics: where genes are and how they got there. *Genome Biol.* [online] (cited 09 March 2001) http://genomebiology.com/2001/2/3/reviews/0002 (2001).
45. Vazquez, J., Belmont, A. S. & Sedat, J. W. Multiple regimes of constrained chromosome motion are regulated in the interphase *Drosophila* nucleus. *Curr. Biol.* **11,** 1227–1239 (2001).
46. Heun, P., Laroche, T., Shimada, K., Furrer, P. & Gasser, S. M. Chromosome dynamics in the yeast interphase nucleus. *Science* **294,** 2181–2186 (2001).
47. Muratani, M. *et al.* Metabolic-energy-dependent movement of PML bodies within the mammalian cell nucleus. *Nature Cell Biol.* **4,** 106–110 (2002).
48. Misteli, T. Protein dynamics: implications for nuclear architecture and gene expression. *Science* **291,** 843–847 (2001).
49. Spector, D. L. Nuclear domains. *J. Cell Sci.* **114,** 2891–2893 (2001).
50. Pederson, T. Protein mobility within the nucleus – what are the right moves? *Cell* **104,** 635–638 (2001).
51. Sheetz, M. P., Turney, S., Qian, H. & Elson, E. L. Nanometre-level analysis demonstrates that lipid flow does not drive membrane glycoprotein movements. *Nature* **340,** 284–288 (1989).
52. Saxton, M. J. Single-particle tracking: the distribution of diffusion coefficients. *Biophys J.* **72,** 1744–1753 (1997).

ACKNOWLEDGEMENTS

We thank M. Saxton for discussions on anomalous diffusion, members of the Lamond lab and P. Nero for helpful discussions. We thank M. Sanders and P. Crews for supplying the latrunculin A preparation, which was supported by National Institutes of Health grant CA47135 to P. Crews. M.P. was supported by a Dame Catherine Cookson studentship and a Biotechnology and Biological Sciences Research Council Studentship. A.I.L. is a Wellcome Trust Principal Research Fellow. J.R.S. is a Wellcome Trust Career Development Fellow (054333).

Correspondence and requests for material should be addressed to J.R.S.

Supplementary information is available on *Nature Cell Biology*'s website (http://cellbio.nature.com).

COMPETING FINANCIAL INTERESTS

The authors declare that they have no competing financial interests.